

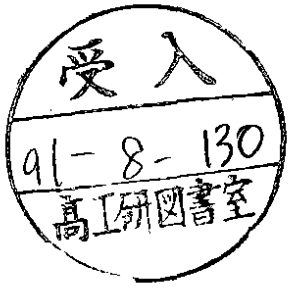
PDF hosted at the Radboud Repository of the Radboud University Nijmegen

The following full text is a preprint version which may differ from the publisher's version.

For additional information about this publication click this link.

<http://hdl.handle.net/2066/125109>

Please be advised that this information was generated on 2021-10-21 and may be subject to change.



EUROPEAN ORGANISATION FOR NUCLEAR RESEARCH

CERN-PPE/91-110

July 9, 1991

A Study of Bose-Einstein Correlations in e^+e^- Annihilations at LEP

The OPAL Collaboration

Abstract

Bose-Einstein correlations between like-sign charged track pairs have been studied in e^+e^- annihilation hadronic events at centre-of-mass energies around the Z^0 peak as a function of Q , the four-momentum difference of the pair. The measurement was performed with the OPAL detector at LEP. Assuming the charged tracks to be pions, the observed Bose-Einstein enhancement was used to extract the values of the strength of the effect and the radius of the pion emitting source, which were found to be $\lambda = 0.866 \pm 0.032 \pm 0.140$ and $R_0 = 0.928 \pm 0.019 \pm 0.150$ fm, respectively, where the first error is statistical and the second is systematic. The results do not show significant variation in comparison to e^+e^- annihilation measurements at lower centre-of-mass energies. If non-pion track contamination is taken into account, the value of the strength λ becomes consistent with unity.

(To be submitted to Physics Letters B)

The OPAL Collaboration

P.D. Acton²⁵, G. Alexander²³, J. Allison¹⁶, P.P. Allport⁵, K.J. Anderson⁹, S. Arcelli², J.C. Armitage⁶,
 P. Ashton¹⁶, A. Astbury^a, D. Axen^b, G. Azuelos^{18,c}, G.A. Bahan¹⁶, J.T.M. Baines¹⁶, A.H. Ball¹⁷,
 J. Banks¹⁶, G.J. Barker¹³, R.J. Barlow¹⁶, J.R. Batley⁵, G. Beaudoin¹⁸, A. Beck²³, J. Becker¹⁰,
 T. Behnke⁸, K.W. Bell²⁰, G. Bella²³, S. Bethke¹¹, O. Biebel³, U. Binder¹⁰, I.J. Bloodworth¹, P. Bock¹¹,
 B. Boden³, H.M. Bosch¹¹, S. Bougerolle^b, B.B. Brabson¹², H. Breuker⁸, R.M. Brown²⁰, R. Brun⁸,
 A. Buijs⁸, H.J. Burckhart⁸, P. Capiluppi², R.K. Carnegie⁶, A.A. Carter¹³, J.R. Carter⁵, C.Y. Chang¹⁷,
 D.G. Charlton⁸, J.T.M. Chrin¹⁶, P.E.L. Clarke²⁵, I. Cohen²³, W.J. Collins⁵, J.E. Conboy¹⁵,
 M. Cooper²², M. Couch¹, M. Coupland¹⁴, M. Cuffiani², S. Dado²², G.M. Dallavalle², S. De Jong⁸,
 P. Debu²¹, L. Del Pozo⁵, M.M. Deninno², A. Dieckmann¹¹, M. Dittmar⁴, M.S. Dixit⁷, E. Duchovni²⁶,
 G. Duckeck¹¹, I.P. Duerdoth¹⁶, D.J.P. Dumas⁶, G. Eckerlin¹¹, P.A. Elcombe⁵, P.G. Estabrooks⁶,
 E. Etzion²³, F. Fabbri², M. Fincke-Keeler^a, H.M. Fischer³, D.G. Fong¹⁷, C. Fukunaga²⁴, A. Gaidot²¹,
 O. Ganel²⁶, J.W. Gary¹¹, J. Gascon¹⁸, R.F. McGowan¹⁶, N.I. Geddes²⁰, C. Geich-Gimbel³,
 S.W. Gensler⁹, F.X. Gentit²¹, G. Giacomelli², V. Gibson⁵, W.R. Gibson¹³, J.D. Gillies²⁰,
 J. Goldberg²², M.J. Goodrick⁵, W. Gorn⁴, C. Grandi², F.C. Grant⁵, E. Gross²⁶, J. Hagemann⁸,
 G.G. Hanson¹², M. Hansroul⁸, C.K. Hargrove⁷, P.F. Harrison¹³, J. Hart⁵, P.M. Hattersley¹,
 M. Hauschild⁸, C.M. Hawkes⁸, E. Heflin⁴, R.J. Hemingway⁶, R.D. Heuer⁸, J.C. Hill⁵, S.J. Hillier¹,
 D.A. Hinshaw¹⁸, C. Ho⁴, J.D. Hobbs⁹, P.R. Hobson²⁵, D. Hochman²⁶, B. Holl⁸, R.J. Homer¹,
 S.R. Hou¹⁷, C.P. Howarth¹⁵, R.E. Hughes-Jones¹⁶, R. Humbert¹⁰, P. Igo-Kemenes¹¹, H. Ihssen¹¹,
 D.C. Imrie²⁵, L. Janissen⁶, A. Jawahery¹⁷, P.W. Jeffreys²⁰, H. Jeremie¹⁸, M. Jimack², M. Jobes¹,
 R.W.L. Jones¹³, P. Jovanovic¹, D. Karlen⁶, K. Kawagoe²⁴, T. Kawamoto²⁴, R.K. Keeler^a,
 R.G. Kellogg¹⁷, B.W. Kennedy¹⁵, C. Kleinwort⁸, D.E. Klem¹⁹, T. Kobayashi²⁴, T.P. Kokott³,
 S. Komamiya²⁴, L. Köpke⁸, R. Kowalewski⁶, H. Kreutzmann³, J. von Krogh¹¹, J. Kroll⁹,
 M. Kuwano²⁴, P. Kyberd¹³, G.D. Lafferty¹⁶, F. Lamarche¹⁸, W.J. Larson⁴, J.G. Layter⁴, P. Le Du²¹,
 P. Leblanc¹⁸, A.M. Lee¹⁷, M.H. Lehto¹⁵, D. Lellouch⁸, P. Lennert¹¹, C. Leroy¹⁸, L. Lessard¹⁸, J. Letts⁴,
 S. Levegrün³, L. Levinson²⁶, S.L. Lloyd¹³, F.K. Loebinger¹⁶, J.M. Lorah¹⁷, B. Lorazo¹⁸, M.J. Losty⁷,
 X.C. Lou¹², J. Ludwig¹⁰, M. Mannelli⁸, S. Marcellini², G. Maringer³, A.J. Martin¹³, J.P. Martin¹⁸,
 T. Mashimo²⁴, P. Mättig³, U. Maur³, J. McKenna^a, T.J. McMahon¹, J.R. McNutt²⁵, F. Meijers⁸,
 D. Menszner¹¹, F.S. Merritt⁹, H. Mes⁷, A. Michelini⁸, R.P. Middleton²⁰, G. Mikenberg²⁶,
 J. Mildener⁶, D.J. Miller¹⁵, C. Milstene²⁴, R. Mir¹², W. Mohr¹⁰, C. Moisan¹⁸, A. Montanari²,
 T. Mori²⁴, M.W. Moss¹⁶, T. Mouthuy¹², B. Nellen³, H.H. Nguyen⁹, M. Nozaki²⁴, S.W. O'Neale^{8,d},
 B.P. O'Neill⁴, F.G. Oakham⁷, F. Odorici², M. Ogg⁶, H.O. Ogren¹², H. Oh⁴, C.J. Oram^e, M.J. Oreglia⁹,
 S. Orito²⁴, J.P. Pansart²¹, B. Panzer-Steindel⁸, P. Paschievici²⁶, G.N. Patrick²⁰, S.J. Pawley¹⁶,
 P. Pfister¹⁰, J.E. Pilcher⁹, J.L. Pinfold²⁶, D.E. Plane⁸, P. Poffenberger^a, B. Poli², A. Pouladdej⁶,
 E. Prebys⁸, T.W. Pritchard¹³, H. Przysiezniak¹⁸, G. Quast⁸, M.W. Redmond⁹, D.L. Rees¹, K. Riles⁴,
 S.A. Robins¹³, D. Robinson⁸, A. Rollnik³, J.M. Roney⁹, E. Ros⁸, S. Rossberg¹⁰, A.M. Rossi^{2,f},
 P. Routenburg⁶, K. Runge¹⁰, O. Runolfsson⁸, D.R. Rust¹², S. Sanghera⁶, M. Sasaki²⁴, A.D. Schaile¹⁰,
 O. Schaile¹⁰, W. Schappert⁶, P. Scharff-Hansen⁸, P. Schenk^a, H. von der Schmitt¹¹, S. Schreiber³,
 J. Schwarz¹⁰, W.G. Scott²⁰, M. Settles¹², B.C. Shen⁴, P. Sherwood¹⁵, R. Shypit^b, A. Simon³,
 P. Singh¹³, G.P. Siroli², A. Skuja¹⁷, A.M. Smith⁸, T.J. Smith⁸, G.A. Snow¹⁷, R. Sobie^g,
 R.W. Springer¹⁷, M. Sproston²⁰, K. Stephens¹⁶, H.E. Stier¹⁰, R. Ströhmer¹¹, D. Strom⁹, H. Takeda²⁴,
 T. Takeshita²⁴, P. Taras¹⁸, S. Tarem²⁶, P. Teixeira-Dias¹¹, N.J. Thackray¹, G. Transtromer²⁵,
 T. Tsukamoto²⁴, M.F. Turner⁵, G. Tysarczyk-Niemeyer¹¹, D. Van den plas¹⁸, R. Van Kooten⁸,
 G.J. VanDalen⁴, G. Vasseur²¹, C.J. Virtue¹⁹, A. Wagner¹¹, C. Wahl¹⁰, J.P. Walker¹, C.P. Ward⁵,
 D.R. Ward⁵, P.M. Watkins¹, A.T. Watson¹, N.K. Watson⁸, M. Weber¹¹, P. Weber⁶, S. Weisz⁸,
 P.S. Wells⁸, N. Wermes¹¹, M. Weymann⁸, M.A. Whalley¹, G.W. Wilson²¹, J.A. Wilson¹, I. Wingter⁸,
 V-H. Winterer¹⁰, N.C. Wood¹⁶, S. Wotton⁸, T.R. Wyatt¹⁶, R. Yaari²⁶, Y. Yang^{4,h}, G. Yekutieli²⁶,
 I. Zacharov⁸, W. Zeuner⁸, G.T. Zorn¹⁷.

- ¹School of Physics and Space Research, University of Birmingham, Birmingham, B15 2TT, UK
- ²Dipartimento di Fisica dell' Università di Bologna and INFN, Bologna, 40126, Italy
- ³Physikalisches Institut, Universität Bonn, D-5300 Bonn 1, FRG
- ⁴Department of Physics, University of California, Riverside, CA 92521 USA
- ⁵Cavendish Laboratory, Cambridge, CB3 0HE, UK
- ⁶Carleton University, Dept of Physics, Colonel By Drive, Ottawa, Ontario K1S 5B6, Canada
- ⁷Centre for Research in Particle Physics, Carleton University, Ottawa, Ontario K1S 5B6, Canada
- ⁸CERN, European Organisation for Particle Physics, 1211 Geneva 23, Switzerland
- ⁹Enrico Fermi Institute and Department of Physics, University of Chicago, Chicago Illinois 60637, USA
- ¹⁰Fakultät für Physik, Albert Ludwigs Universität, D-7800 Freiburg, FRG
- ¹¹Physikalisches Institut, Universität Heidelberg, Heidelberg, FRG
- ¹²Indiana University, Dept of Physics, Swain Hall West 117, Bloomington, Indiana 47405, USA
- ¹³Queen Mary and Westfield College, University of London, London, E1 4NS, UK
- ¹⁴Birkbeck College, London, WC1E 7HV, UK
- ¹⁵University College London, London, WC1E 6BT, UK
- ¹⁶Department of Physics, Schuster Laboratory, The University, Manchester, M13 9PL, UK
- ¹⁷Department of Physics and Astronomy, University of Maryland, College Park, Maryland 20742, USA
- ¹⁸Laboratoire de Physique Nucléaire, Université de Montréal, Montréal, Quebec, H3C 3J7, Canada
- ¹⁹National Research Council of Canada, Herzberg Institute of Astrophysics, Ottawa, Ontario K1A 0R6, Canada
- ²⁰Rutherford Appleton Laboratory, Chilton, Didcot, Oxfordshire, OX11 0QX, UK
- ²¹DPhPE, CEN Saclay, F-91191 Gif-sur-Yvette, France
- ²²Department of Physics, Technion-Israel Institute of Technology, Haifa 32000, Israel
- ²³Department of Physics and Astronomy, Tel Aviv University, Tel Aviv 69978, Israel
- ²⁴International Centre for Elementary Particle Physics and Dept of Physics, University of Tokyo, Tokyo 113, and Kobe University, Kobe 657, Japan
- ²⁵Brunel University, Uxbridge, Middlesex, UB8 3PH UK
- ²⁶Nuclear Physics Department, Weizmann Institute of Science, Rehovot, 76100, Israel
- ^aUniversity of Victoria, Dept of Physics, P O Box 3055, Victoria BC V8W 3P6, Canada
- ^bUniversity of British Columbia, Dept of Physics, 6224 Agriculture Road, Vancouver BC V6T 1Z1, Canada
- ^cAlso at TRIUMF, Vancouver, Canada V6T 2A3
- ^dOn leave from Birmingham University, Birmingham B15 2TT, UK
- ^eUniv of Victoria, Dept of Physics, P.O. Box 1700, Victoria BC V8W 2Y2, Canada and TRIUMF, Vancouver, Canada V6T 2A3
- ^fPresent address: Dipartimento di Fisica, Università della Calabria and INFN, 87036 Rende, Italy
- ^gUniversity of British Columbia, Dept of Physics, 6224 Agriculture Road, Vancouver BC V6T 2A6, Canada and IPP, McGill University, High Energy Physics Department, 3600 University Str, Montreal, Quebec H3A 2T8, Canada
- ^hOn leave from Research Institute for Computer Peripherals, Hangzhou, China
- ⁱOn leave from Tel Aviv University, Tel Aviv, Israel

1 Introduction

The interference between like-sign pions was first investigated in the late 1950's by Goldhaber, Goldhaber, Lee and Pais [1] in $p\bar{p}$ annihilations, and was interpreted to be a consequence of Bose-Einstein (BE) statistics obeyed by identical pion pairs. The effect resulted in an enhancement of the number of like-sign charged track pairs compared to unlike-sign charged pairs when the two particles had similar momenta, i.e. identical bosons tended to be emitted close to each other in phase space. Since then, BE correlations have been observed over a wide range of centre-of-mass energies in hadronic collisions, lepton-hadron collisions, as well as in e^+e^- interactions [2 - 14].

The theory of BE correlations is described in refs. [15], [16]. The BE correlations can be described in terms of a correlation function C defined by:

$$C(p_1, p_2) = \frac{\rho(p_1, p_2)}{\rho_0(p_1, p_2)} \quad (1)$$

where p_1 and p_2 are the four-momenta of the two tracks, $\rho(p_1, p_2) = (1/\sigma)(d^8\sigma/d^4p_1 d^4p_2)$ is the measured density for two identical bosons, and $\rho_0(p_1, p_2)$ is the two-particle density in the absence of BE correlations.

Various types of parametrisations of the BE correlation function can be found in the literature [17],[18], which usually refer to the overall centre-of-mass reference frame. In the Lorentz invariant parametrisation, the correlation function C is studied as a function of the four-momentum difference of the pair $Q^2 = -(p_1 - p_2)^2$, which, if both particles are assumed to be pions, can be expressed as $Q^2 = M^2 - 4m_\pi^2$, where M is the invariant mass of the pair. If the pion source is assumed to have a Gaussian shape in the rest frame of the pion pair, $C(Q)$ can be parametrised as $C(Q) = 1 + e^{-Q^2 R^2}$, where the parameter R is related to the size R_0 of the pion emitter through the relation $R_0 = Rhc$. The parameter R_0 can be interpreted as being the size of the region from which pions of similar momenta are emitted [19].

The correlation function $C(Q)$ is predicted to have the value 1 at $Q = 0$ in the absence of the BE effect and the value 2 in its presence. Experiments have reported values of $C(Q = 0)$ between 1 and 2 (refs. [2 - 14]). This can be interpreted to mean that the BE effect does not affect all particles in the final state, since particle emission can occur from partially coherent systems rather than from purely incoherent ones. In addition, not all particle pairs are formed from identical bosons, which contributes to a further decrease of the enhancement at $Q = 0$. To take these factors into account, the correlation function usually includes an additional parameter λ , which represents the "strength" of the effect and which assumes values between 0 and 1, such that $C(Q)$ becomes:

$$C(Q) = 1 + \lambda e^{-Q^2 R^2} \quad (2)$$

The parameter λ is often called the "chaoticity parameter".

To fit our data, we used the following expression for the BE correlation function:

$$C(Q) = N (1 + \lambda e^{-Q^2 R^2}) (1 + \delta Q + \epsilon Q^2) \quad (3)$$

where N is a normalisation factor and the term $(1 + \delta Q + \epsilon Q^2)$ is an empirical term which takes into account the rise of the correlation function at large values of Q , due to long range correlations between particle pairs (e.g. charge and energy conservation, phase-space constraints, etc.). Other experiments use alternatively terms which are only linear or quadratic in Q . Although these expressions are purely empirical, they have been shown to describe data well over a wide range of energies (refs. [2 - 14]).

A crucial feature of the measurement is the choice of the reference sample $\rho_0(p_1, p_2)$. Ideally it should satisfy the following conditions:

- 1) absence of BE correlations;
- 2) presence of correlations due to energy-momentum and charge conservation;
- 3) presence of correlations due to the topology and the global properties of the events;
- 4) absence of additional dynamical correlations due to resonances or long-lived particle decays.

In this analysis the reference sample was computed by taking unlike-sign pair combinations in an event. This method satisfies conditions 1), 2) and 3) but not condition 4). The reference sample computed in this way is thus obtained entirely from data, but it is affected by the presence of dynamical correlations due to resonances or long-lived particle decays (especially K^0 , ρ^0 and η). This may introduce systematic effects into the correlation function. In section 3 we discuss the impact that the resonances in the reference sample have on the results.

In this analysis 146624 multi-hadronic Z^0 candidates were used, collected by the OPAL detector during the 1990 LEP running period at centre-of-mass energies between 88 and 94 GeV. The mean centre-of-mass energy was 91.3 GeV. Our analysis also makes use of a Monte Carlo simulation of this data sample, as discussed below.

The Monte Carlo generator used to simulate multi-hadronic Z^0 decays was Jetset 7.2 [20]. This generator is able to simulate the characteristics of the final states with good accuracy [21]. The Monte Carlo program also included a detailed description of the detector geometry and material as well as effects of the detector resolution and efficiencies [22]. It produced an output identical in format to that of the detector data acquisition system, such that simulated data could be processed by the same analysis chain as real events. The BE effect can be simulated in Jetset 7.2 as an option, which by default is not enabled, by setting ad-hoc parameters. In section 5 we present values for the Jetset parameters which describe our measurement of the BE interference.

2 Detector and Data Selection

The OPAL detector has been described in detail in reference [23]. The present analysis is based mainly on information from the central tracking chambers, consisting of a vertex chamber, a jet chamber and a chamber for measurements in the z direction (z is the coordinate parallel to the beam axis), all enclosed by a solenoidal magnet coil which produces an axial field of 0.435 T. The main tracking detector is the jet chamber, which has a length of 4 m, a diameter of 3.7 m and which provides up to 159 space points and close to 100% track-finding efficiency for charged tracks in the region $|\cos\theta| < 0.92$, where θ is the polar angle. The momentum resolution, which is of particular relevance for this analysis, can be parametrised as $\Delta p/p^2 \approx 2.2 \cdot 10^{-3} \text{ GeV}^{-1}$. The jet chamber is also able to perform particle identification by energy loss dE/dx measurements with a resolution $\sigma(dE/dx)/(dE/dx) \approx 3.8\%$. The trigger and on-line event selection for hadronic events are described in reference [24]. Additional criteria were used for this analysis to select well measured and well contained events in the tracking detector, as described below.

Charged tracks were accepted if their extrapolated closest distance of approach to the interaction point was less than 1 cm in the plane perpendicular to the beam axis and less than 15 cm in the direction along the beam axis. The tracks were required to have at least 40 hits in the jet chamber and the first hit had to be closer than 70 cm to the beam axis. For each track the transverse momentum relative to the beam axis had to be larger than 0.15 GeV and the polar angle θ_{track} had to satisfy $|\cos\theta_{track}| < 0.94$.

The total visible momentum, defined as the scalar sum of the momenta of the charged tracks which passed the cuts, was required to be at least 10% of the centre-of-mass energy. Events with an observed charged-track multiplicity $n_{\text{ch}} < 5$ were rejected, in order to eliminate tau-pairs and two-photon events. The angle of the thrust axis, computed using the tracks which passed the cuts, had to satisfy $|\cos\theta_{\text{thrust}}| < 0.82$. The event was also rejected if any outgoing track had a measured momentum larger than the beam momentum. This last cut affected less than 1% of the events.

Tracks used in pair combinations for the analysis were required to have a momentum smaller than 10 GeV, since particle correlations may be influenced by phase-space limitations, and an estimated absolute error on the track momentum which was smaller than 0.1 GeV. Finally, tracks were required to have at least 60 space point measurements in the jet chamber.

Electron pairs from photon conversions might strongly affect the Q distribution of unlike-sign pairs, and thus the reference sample, in the region of low values of Q . The mean energy loss for electrons is expected to be $\langle dE/dx \rangle_e = 9.7 \text{ keV/cm}$, with a resolution of $\sigma_{dE/dx} \approx 0.4 \text{ keV/cm}$. Therefore, to reject electrons, tracks used in the pair combinations were required to have dE/dx values smaller than 9 keVcm^{-1} . In addition, pairs were rejected if their invariant mass (assuming both tracks to be pions) was smaller than 0.4 GeV and if their opening angle in the plane orthogonal to the beam axis was smaller than 0.1 rad. These cuts were applied to both like- and unlike-sign pairs in order to avoid a bias in the data selection. A vertex finding algorithm was used to further improve the rejection. The intersection points of track pairs in the radial plane were considered to be candidate secondary vertices. Tracks were rejected if their intersection point had a radial distance larger than 1 cm from the primary vertex. This cut also helped to reject pion pairs from K^0 decays. After these cuts the efficiency for rejecting electrons was estimated from Monte Carlo to be better than 99%.

After the cuts described above, the event was rejected if the difference between the number of positive and negative tracks exceeded 25% of the total number of charged tracks. This cut was required in order to keep balanced the number of like- and unlike-sign pairs in an event and eliminated 9% of the data sample.

Starting from an initial sample of 146624 multi-hadronic Z^0 decays, 76841 events passed the cuts and were used for the analysis.

3 Systematic Effects, Corrections and Results

The correlation function $C(Q)$ derived using the method described in section 1 is shown in Fig. 1, for both data and Monte Carlo (where the BE effect is not simulated). A clear enhancement at low values of Q is observed in the data. The distortion of the correlation function in the range $0.3 < Q < 0.9 \text{ GeV}$, visible for both Monte Carlo and data, is introduced by dynamical correlations in the reference sample due to unlike-sign pairs coming mainly from K^0 and ρ^0 decays. In addition, the Monte Carlo correlation function exhibits a small rise for $Q \approx 0$ because of η' and η decays. These effects will be discussed in more detail below.

Coulomb interactions between particles affect like- and unlike-sign pairs in opposite ways and modify the correlation function. A correction for Coulomb interactions was applied to the correlation function as a function of Q [16]. The corrected correlation function is:

$$C_{\text{corr}}(Q) = \chi(Q)C_{\text{uncorr}}(Q) \quad (4)$$

where $\chi(Q)$ is:

$$\chi(Q) = \frac{e^{2\pi\eta} - 1}{1 - e^{-2\pi\eta}} \quad (5)$$

with $\eta = \alpha m_\pi / \sqrt{Q^2}$ and α the fine-structure constant. The correction factor $\chi(Q)$ is of the order of a few percent for $Q < 0.2$ GeV and is negligible for larger Q . The corrected correlation function is shown in Fig. 2, by the black dots.

A considerable fraction of the final-state pions in multihadron events originates from decays of long-lived particles. Here we define a long-lived particle to be one which has a long flight distance compared to the typical correlation length of BE interference (which is of the order of 1 fm), so that it decays far away from the region where most pions are produced. Such long-lived particles include the η , η' and ω , as well as hadrons containing heavy quarks. These particles contribute to the BE effect only at very small values of Q , of the order of their decay width, and they produce a narrow spike in the correlation function at $Q \approx 0$ [19]. The range $Q < 0.05$ GeV is excluded from our analysis, so that the contribution of pions coming from the same long-lived particle decay is mostly eliminated. Pairs which contain one pion from a long-lived particle decay or pions from two different long-lived particle decays should not exhibit any BE effect, leading to a reduction in the observed value of λ . This effect could be large, of the order of 40% or more, because of the large number of pions from long-lived particles: as a consequence, an underestimate of λ of this same order of magnitude could be expected [19]. This is contradicted by experimental measurements of λ , which are not consistent with such a large effect (refs. [4],[11]), thus suggesting that the effect of long-lived resonances in BE interference is not well understood or that other effects might compensate it [12]. No correction was applied for this effect.

In the case of η and η' decays, a further effect was observed. For about 15% of the pion like-sign pairs, at least one of the charged tracks arises from the decay chain $\eta' \rightarrow \pi^+\pi^-\eta$ followed by $\eta \rightarrow \pi^+\pi^-\pi^0$. These pairs are not uniformly distributed in Q . Monte Carlo simulation shows that their four-momentum difference tends to be small, with a sharp peak at $Q < 0.075$ GeV, because of kinematic constraints due to the limited phase space available to the pions. This produces a fake enhancement of the correlation function, which is estimated from Monte Carlo to be of the order of 10% in the range $Q < 0.075$ GeV. Again, no correction was applied for this effect.

Tracks split into two or more pieces by the reconstruction program could produce a fake rise of the correlation function at low values of Q . The stringent requirements on the quality of the tracks discussed in section 2 are expected to reject most of these split tracks: from Monte Carlo simulation, the fraction of such tracks, after the cuts, is found to be smaller than 10^{-4} and the distribution of their four-momentum difference Q drops to zero for $Q > 0.1$ GeV. The small contamination of fake like-sign pairs due to split tracks is mostly confined to the region $Q < 0.05$ GeV and is therefore excluded from our analysis, since we examine pairs with $Q > 0.05$ GeV only, as mentioned above.

To extract values for the correlation strength λ and size R_0 , the correlation function was fitted using expression (3), corrected for Coulomb interaction as in (4), in the range $0.05 < Q < 2$ GeV, with the exclusion of the ranges $0.35 < Q < 0.45$ GeV and $0.6 < Q < 0.85$ GeV to avoid the K^0 and ρ^0 regions (fit (a) of Tab. 1). In the following, this fit is referred to as the "reference fit". The parameters obtained from this fit, with their statistical errors, are:

$$\lambda = 0.866 \pm 0.032 \quad R_0 = 0.928 \pm 0.019 \text{ fm}$$

$$\delta = 0.474 \pm 0.050 \text{ GeV}^{-1} \quad \epsilon = -0.120 \pm 0.015 \text{ GeV}^{-2} \quad N = 0.635 \pm 0.025$$

yielding $\chi^2/\text{DOF} = 1.8$. The results of this fit are shown by the solid curve in Fig. 2. The data points

in the range $Q < 0.1$ GeV lie somewhat above the curve, probably because of pions from η' and η decays as discussed above.

If the fit is performed in the more restricted interval $0.05 < Q < 1.5$ GeV, again excluding the K^0 and ρ^0 regions, the parameters λ and R_0 do not change within their statistical errors (fit (b) of Tab. 1). If the fit is made in the region $0.05 < Q < 2$ GeV including the K^0 and ρ^0 regions, the value of λ again remains essentially stable, while R_0 decreases by 14% as reported by fit (c) of Tab. 1.

To estimate systematic effects related to the track and event selection, the analysis was repeated after changing the criteria from those given in section 2. The results were found to be fairly insensitive to the track and event selection criteria which were adopted. The largest variation in the results, for the different sets of cuts which were tested, occurred for the following conditions: the distance of closest approach to the collision point was smaller than 0.7 cm in the r - ϕ plane and 9 cm in the beam direction; the first hit in the jet chamber was less than 30 cm from the beam axis; the transverse momentum of each track was larger than 0.25 GeV and the polar angle θ_{track} satisfied $|\cos \theta_{track}| < 0.9$; the scalar sum of the momenta of the particles exceeded 20% of the centre-of-mass energy. The results obtained for these criteria are given as fit (d) in Tab. 1.

We do not expect effects related to detector acceptance or resolution to be a significant source of systematic error, since these apply equally to both the signal density $\rho(p_1, p_2)$ and the reference density $\rho_0(p_1, p_2)$ of Eq. (1). A small difference between ρ and ρ_0 could arise from a different acceptance for like- and unlike-sign pairs with small opening angles. In the magnetic field, like-sign tracks are deflected in the same direction, while unlike-sign tracks are deflected in opposite directions. Monte Carlo studies showed that there was not a significant difference in acceptance for the two charged track pair types, however this was tested in addition using data, by requiring that the angle between two tracks be larger than 3 degrees, and checking that the results of the fit remained stable.

The momentum resolution is another potential source of systematic error, since poor momentum resolution smears the correlation function. In this analysis the Q resolution estimated from Monte Carlo was found to be better than 0.025 GeV for both the like- and unlike-sign pairs, independent of the direction of the tracks and of the relative sign of the charges of the pairs. For data the Q resolution is expected to be slightly worse. Since the range of the BE correlation is of the order of hundreds of MeV, this effect is assumed to be negligible. The bin size was chosen to be 0.025 GeV, so as to match the estimated Q resolution. Varying the bin size in the range from 0.015 to 0.05 GeV produced changes in the parameters which were smaller than their statistical errors. The largest variation from the reference fit occurred when the bin width was chosen to be 0.05 GeV. The results for this fit are given as entry (e) of Tab. 1.

Contamination of the charged track sample by particles other than pions is a large systematic effect. Monte Carlo simulation yields an estimated purity of the $\pi\pi$ sample of about 80%, the background being mainly $K\pi$ and $p\pi$ pairs. This is expected to lead to an underestimate of λ of about 20%. This can be better expressed by the following relation [13]:

$$C(Q) = N (1 + f(Q)) \lambda e^{-Q^2 R^2} (1 + \delta Q + \epsilon Q^2) \quad (6)$$

where $C(Q)$ is the correlation function (3) corrected for Coulomb interactions and modified by the presence of the term $f(Q)$ which is the fraction of like-sign $\pi\pi$ pairs, estimated from Monte Carlo simulation. The function $f(Q)$, for our case, appears to have a slight pair mass dependence, which we parametrised as $f(Q) = 0.81 - 0.07Q$ in the range $0.05 < Q < 2$ GeV. Fitting expression (6) to our measurements yields the results summarised by fit (f) in Tab. 1. As expected, R_0 is almost insensitive to the correction for non-pion contamination, while λ assumes the value 1.078 ± 0.050 which is consistent with maximal strength $\lambda = 1$. This result depends on the reliability of the Monte

Carlo simulation. A cross check using data was made by repeating the track-selection using the dE/dx measurement in order to select pions. The Monte Carlo gave in this case a probability of 93% for having true $\pi\pi$ pairs, with a very small Q -dependence. The data were fitted to equation (3), corrected for Coulomb interactions as in equation (4), without the term $f(Q)$ introduced for equation (6). The strength of the correlation was found to be $\lambda = 0.943 \pm 0.050$ whereas R_0 remained stable within the statistical error.

To estimate the sensitivity of the results on the choice of the reference sample, we employed a second technique to calculate this sample, based on the Monte Carlo simulation. The Monte Carlo does not include the BE effect, but includes the other relevant dynamical correlations present in the real data. Dividing the data correlation function corrected for Coulomb interactions of Fig. 2 by the Monte Carlo one of Fig. 1b¹, a new correlation function

$$C'(Q) = \frac{N_{\text{like}}^{\text{data}}/N_{\text{unlike}}^{\text{data}}}{N_{\text{like}}^{\text{MC}}/N_{\text{unlike}}^{\text{MC}}} \quad (7)$$

is obtained which contains only the BE enhancement, assuming factorisation. This method, although fully dependent on the quality of the simulation, should correct for the correlations introduced by the K^0 and ρ^0 . It should also correct for the slow variation of the correlation function seen at large values of Q in Fig. 2. The results of the fit, performed over the complete range $0.05 < Q < 2$ GeV, are given in fit (g) of Tab. 1. The measured correlation function (7) is plotted in Fig. 3. The solid curve in this figure shows the results of the fit. It is interesting that this method yields a better fit to the data for very low values of Q , than was obtained for the correlation function based on data only (Fig. 2). This is possibly because the background contributions at small Q values from η' and η decays are present in both data and Monte Carlo. The difference in the results obtained from the two methods, the one based on Monte Carlo and the other based on data, is taken as a contribution to the overall systematic error.

A systematic uncertainty in the values of the parameters may arise from the choice of the term which describes the behaviour of the correlation function at large Q . The expression

$$C(Q) = N(1 + \lambda e^{-Q^2 R^2})(1 + \delta Q) \quad (8)$$

has been used by other experiments to fit the data, as an alternative to expression (3). This parametrisation is linear in Q for large Q values. Fit (h) in Tab. 1 gives the result we obtained when expression (8) was used in place of expression (3). Again the Coulomb correction (4) was applied and the fit was performed excluding the K^0 and ρ^0 regions. We observed variations in the values of λ and R_0 of the order of 10% and 14% respectively, compared to the fit to Eq. (3). However, the fit to equation (8) does not reproduce our data properly at large values of Q , and this results in a large value of χ^2/DOF , as shown in Tab. 1.

The results from the various fits for the parameters R_0 and λ are summarised in Tab. 1, where fit (a) is taken as the reference. Fits (b), (c), (d), (e) and (g) are used to evaluate the overall systematic errors. They are computed by summing in quadrature the difference in the parameter values which are observed relative to the reference fit. The final values of the parameters λ and R_0 are:

$$\lambda = 0.866 \pm 0.032 \pm 0.140 \quad R_0 = 0.928 \pm 0.019 \pm 0.150 \text{ fm}$$

where the first error is statistical and the second is systematic. The errors are dominated by the systematic ones. The main contribution to the systematic errors comes from the choice of the reference

¹The Monte Carlo does not take into account Coulomb interactions, so that it does not need to be corrected for this effect.

sample and from the differences which are observed when the K^0 and ρ^0 regions are included or excluded.

It is interesting to investigate whether the strength and size of the BE correlations are related to the multiplicity of the event. To study this we analysed two subsets of events with charged-particle multiplicity values $n_{ch} \leq 17$ and $n_{ch} \geq 18$, yielding mean multiplicity values of $\langle n_{ch} \rangle = 10.1$ and $\langle n_{ch} \rangle = 23.2$, respectively. A small decrease of λ and a small increase of R_0 were observed, going from the set with lower multiplicity to that with higher one, as reported in fits (i) and (j) of Tab. 1. Although more careful studies are needed, this is in qualitative agreement with results obtained by other experiments [8].

Comparison with other experiments is not straightforward, since different corrections for systematic effects and different parametrisations for the BE correlation function have been used. Nonetheless, our measurements of λ and R_0 are not significantly different from those obtained by e^+e^- experiments at lower centre-of-mass energies, as shown in Fig. 4. The errors are statistical and systematic (added in quadrature) in the case of OPAL whereas they are statistical only for the other experiments. The results shown for R_0 in Fig. 4 seem to exclude the possibility that the source size increases with the energy [13]. The value of R_0 can be interpreted as being the average size of local regions where the pions are produced rather than as being the size of the entire hadronization region [11], [19]. This could explain why its value of about 1 fm is rather independent of the centre-of-mass energy and also the fact that similar values to these e^+e^- ones are obtained in other types of collisions, such as neutrino-nucleon or muon-nucleon collisions. In the case of hadron-hadron collisions the size of the emitter is also of the size of 1 fm, although these latter experiments generally report values which are slightly larger than for the other types of collisions [8].

4 Monte Carlo Simulation of the BE Effect

The effect of BE interference can be simulated in Jetset 7.2 by calling the subroutine "LUBOEI" and by setting a few *ad-hoc* parameters in the program ². Monte Carlo events generated with the BE interference were analysed using simulation of the detector and the same track and event criteria described in section 2. The resulting Monte Carlo correlation function was then fitted by equation (3), excluding the K^0 and ρ^0 regions. The parameters of the generator were tuned in order to reproduce the values of λ and R_0 obtained for fit (a) of Tab. 1. The Monte Carlo correlation function obtained in this way is shown in Fig. 2, by the open circles ³.

5 Conclusions

Bose-Einstein correlations have been observed in e^+e^- annihilations into hadrons with the OPAL detector at LEP, at a mean centre-of-mass energy value of 91.3 GeV. Starting from an initial sample of 146624 hadronic decays of the Z^0 , we obtained a strength of the effect $\lambda = 0.866 \pm 0.032 \pm 0.140$ and a size of the pion emitting region $R_0 = 0.928 \pm 0.019 \pm 0.150$ fm which are in agreement with results

²Due to an error in the code of the routine LUBOEI in Jetset 7.2, the corresponding Jetset 7.3 version of this routine was used.

³The parameters of the generator which were changed from their default values, in order to obtain this result, were MSTJ(51)=2, MSTJ(52)=9, PARJ(92)=2.5 and PARJ(93)=0.33 GeV. The effective strength of BE effect is represented by the parameter MSTJ(92). The fact that it is considerably larger than unity is perhaps because of approximations made in the Monte Carlo implementation of the BE correlations.

from e^+e^- experiments at lower centre-of-mass energies. The strength λ assumes a value consistent with unity when the contamination of non-pion tracks is taken into account. This does not leave much room for other effects which could reduce the value of λ , e.g. coherent emission or final-state strong interactions between particles.

6 Acknowledgments

It is a pleasure to thank the SL Division for the efficient operation of the LEP accelerator and its continuing close cooperation with our experimental group. In addition to the support staff at our own institutions we are pleased to acknowledge the following :

Department of Energy, USA

National Science Foundation, USA

Science and Engineering Research Council, UK

Natural Sciences and Engineering Research Council, Canada

Israeli Ministry of Science

Minerva Gesellschaft

The Japanese Ministry of Education, Science and Culture (the Monbusho) and a grant under the Monbusho International Science Research Program

American Israeli Bi-national Science Foundation

Direction des Sciences de la Matière du Commissariat à l'Energie Atomique, France

The Bundesministerium für Forschung und Technologie, FRG

and The A.P. Sloan Foundation.

References

- [1] G. Goldhaber, S. S. Goldhaber, W. Lee, A. Pais, Phys. Rev. Lett. **3** (1959) 181;
G. Goldhaber, S. S. Goldhaber, W. Lee, A. Pais, Phys. Rev. **120** (1960) 300.
- [2] A. Giovannini et al., Riv. Nuovo Cimento **2** (1979) 1.
- [3] M. Deutschmann et al., Nucl. Phys. **B204** (1982) 333.
- [4] P. Avery et al. (CLEO Collaboration), Phys. Rev. **D32** (1985) 2294.
- [5] A. Breakstone et al. (SFM Collaboration), Phys. Lett. **B162** (1985) 400.
- [6] H. Aihara et al. (TPC Collaboration), Phys. Rev. **D31** (1985) 996.
- [7] M. Arneodo et al. (EMC Collaboration), Z. Phys. **C32** (1986) 1.
- [8] B. Lorstad, Int. J. Mod. Phys. **A4** (1989) 2861.
- [9] D. Allasia et al. (WA25 Collaboration), Z. Phys. **C37** (1988) 551.
- [10] M. Althoff et al. (TASSO Collaboration), Z. Phys. **C30** (1986) 355.
- [11] I. Juricic et al. (MARKII Collaboration), Phys. Rev. **D39** (1989) 1.
- [12] G. Goldhaber, "The GGLP Effect Alias B-E Effect Alias H-BT effect", LBL 29494 (1990).
- [13] R. Walker et al. (AMY Collaboration), "B-E Correlations in Pion Production at TRISTAN", KEK Preprint 90-60-AMY 90-5.
- [14] D. H. Boal et al., Rev. of Mod. Phys. **62** (1990) 553.
- [15] W. Hofmann, "A Fresh Look at Bose-Einstein Correlations", LBL 23108 (1987);
M. I. Podgoretskii, Sov. J. Part. Nucl. **20** (1989) 266.
- [16] M. Gyulassy et al., Phys. Rev. **C20** (1979) 2267.
- [17] G. Kopylev and M. Podgoretzki, Sov. J. Nucl. Phys. **18** (1974) 336.
- [18] G. Cocconi, Phys. Lett. **B49** (1974) 459.
- [19] M. G. Bowler, Particle World (Gordon and Breach Science Publishers-Geneve), **2** (1991) 1.
- [20] T. Sjöstrand, Comp. Phys. Comm. **39** (1986) 347;
T. Sjöstrand and M. Bengtsson, Comp. Phys. Comm. **43** (1987) 367.
- [21] M. Z. Akrawy et al. (OPAL Collaboration), Z. Phys. **C47** (1990) 505.
- [22] J. Allison et al., Comp. Phys. Comm. **47** (1987) 55;
R. Brun et al., "GEANT 3" Report DD/EE/84-1 CERN (1989);
D. R. Ward, Proceedings of the MC'91 Workshop, NIKHEF, Amsterdam, 1991.
- [23] K. Ahmet et al. (OPAL Collaboration), "The OPAL Detector at LEP", CERN PPE/90-114,
submitted to Nucl. Instr. and Meth.
- [24] M. Z. Akrawy et al. (OPAL Collaboration), Phys. Lett. **B240** (1990) 497.

Type of fit	λ	$R_0(\text{fm})$	χ^2/DOF
a) Reference fit	0.866 ± 0.032	0.928 ± 0.019	112/61
b) Upper limit of the Q-range, $Q=1.5$ GeV	0.833 ± 0.032	0.946 ± 0.020	106/41
c) Fit including K^0 and ρ^0 regions	0.846 ± 0.025	0.795 ± 0.015	336/73
d) Different data selection	0.881 ± 0.043	0.868 ± 0.025	73/61
e) Use 0.05 GeV binning	0.875 ± 0.030	0.922 ± 0.019	48/28
f) Correction for non $\pi\pi$ pairs	1.078 ± 0.050	0.923 ± 0.019	116/61
g) Data divided by Monte Carlo	0.730 ± 0.036	0.909 ± 0.027	98/61
h) Fit to parametrisation (8)	0.782 ± 0.035	1.054 ± 0.024	242/62
i) Observed charged multiplicity $n_{ch} \leq 17$	0.946 ± 0.056	0.875 ± 0.031	110/61
j) Observed charged multiplicity $n_{ch} \geq 18$	0.816 ± 0.038	0.955 ± 0.025	80/61

Table 1: Results of various fits. Fit (a) is the reference one, obtained by fitting the data to expression (3), corrected for the Coulomb interaction, in the range $0.05 < Q < 2$ GeV with the exclusion of the regions $0.35 < Q < 0.45$ GeV and $0.6 < Q < 0.85$ GeV to avoid the K^0 and ρ^0 resonances. Fit (b) reports the values of the parameters when the upper value of the Q-range was chosen to be $Q = 1.5$ GeV. Fit (c) reports the results when the regions $0.35 < Q < 0.45$ GeV and $0.6 < Q < 0.85$ GeV were included. Fit (d) was obtained by changing the event and track selection. Fit (e) shows the results when a wider bin-width (0.05 GeV) was chosen. Fit (f) reports the case when data were corrected for the presence of non-pion pairs as in Eq. (6). Fit (g) shows the results when Monte Carlo was used, as a second means, to obtain the reference sample. Fit (h) reports the results when a linear rise of the correlation function at large values of Q is chosen, as in Eq. (8). Fits (i) and (j) refer to data samples with observed charged multiplicity $n_{ch} \leq 17$ and $n_{ch} \geq 18$, respectively. The variations of the parameters from fits (b), (c), (d), (e) and (g), with respect to fit (a), were added in quadrature to define the overall systematic error.

Figure Captions

Figure 1 Correlation function C for like-sign pairs relative to unlike-sign pairs as a function of Q for (a) uncorrected data and (b) Jetset 7.2 Monte Carlo with detector simulation and without BE correlations.

Figure 2 Correlation function corrected for the Coulomb interaction as a function of Q . The black circles show the data, and the solid line represents the fit to Eq. (3). The fit is performed excluding the regions of the K^0 and ρ^0 . The open circles show the Monte Carlo correlation function when the BE effect is simulated. The parameters of the generator were tuned to reproduce the measured BE correlations.

Figure 3 Correlation function corrected for the Coulomb interactions divided by the Monte Carlo correlation function as a function of Q . The line represents the fit to Eq. (3).

Figure 4 The radius of the emitting region R_0 and the strength parameter λ from various e^+e^- experiments versus centre-of-mass energy. The errors are statistical and systematic in the case of OPAL and statistical only for the other experiments.

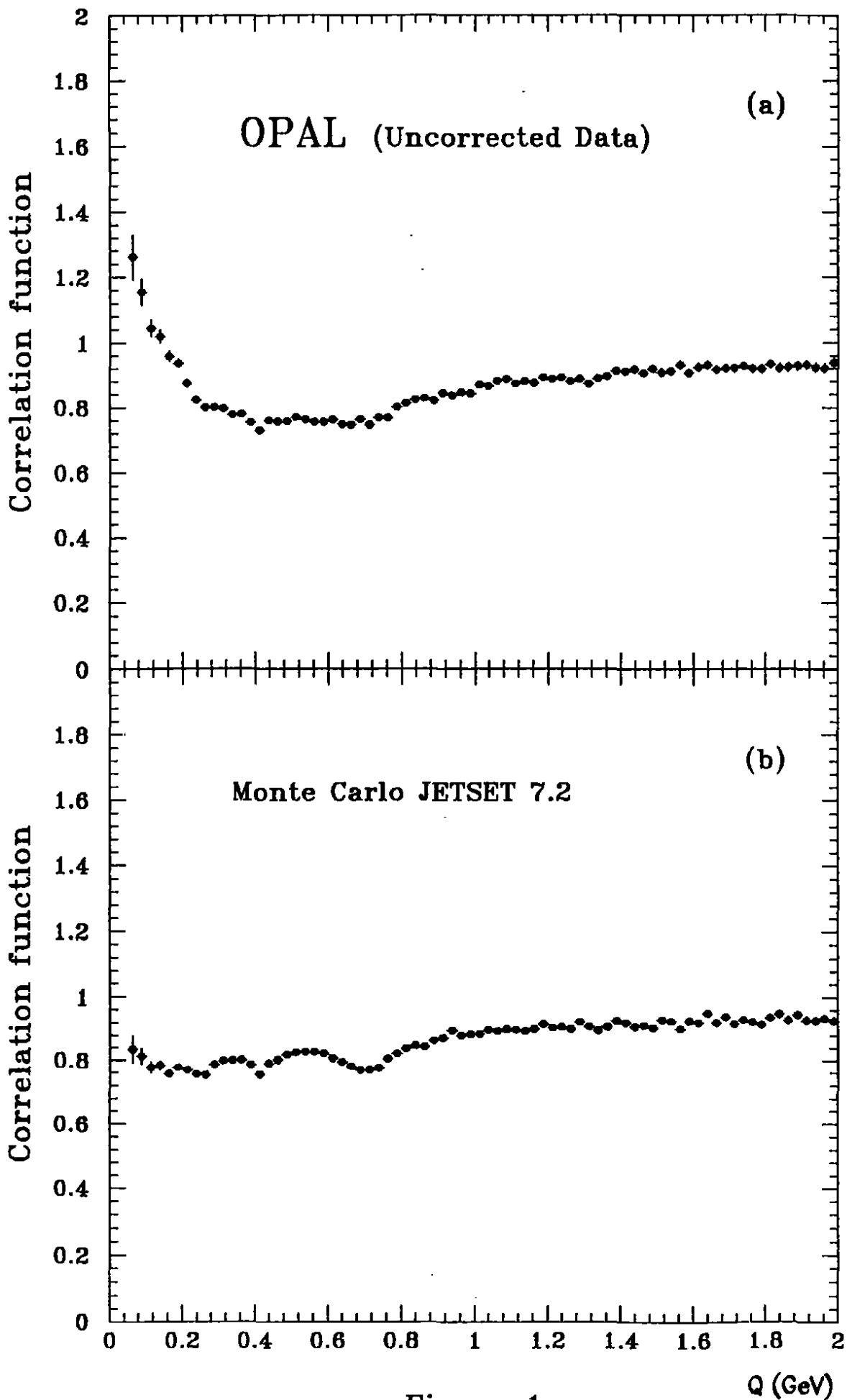


Figure 1

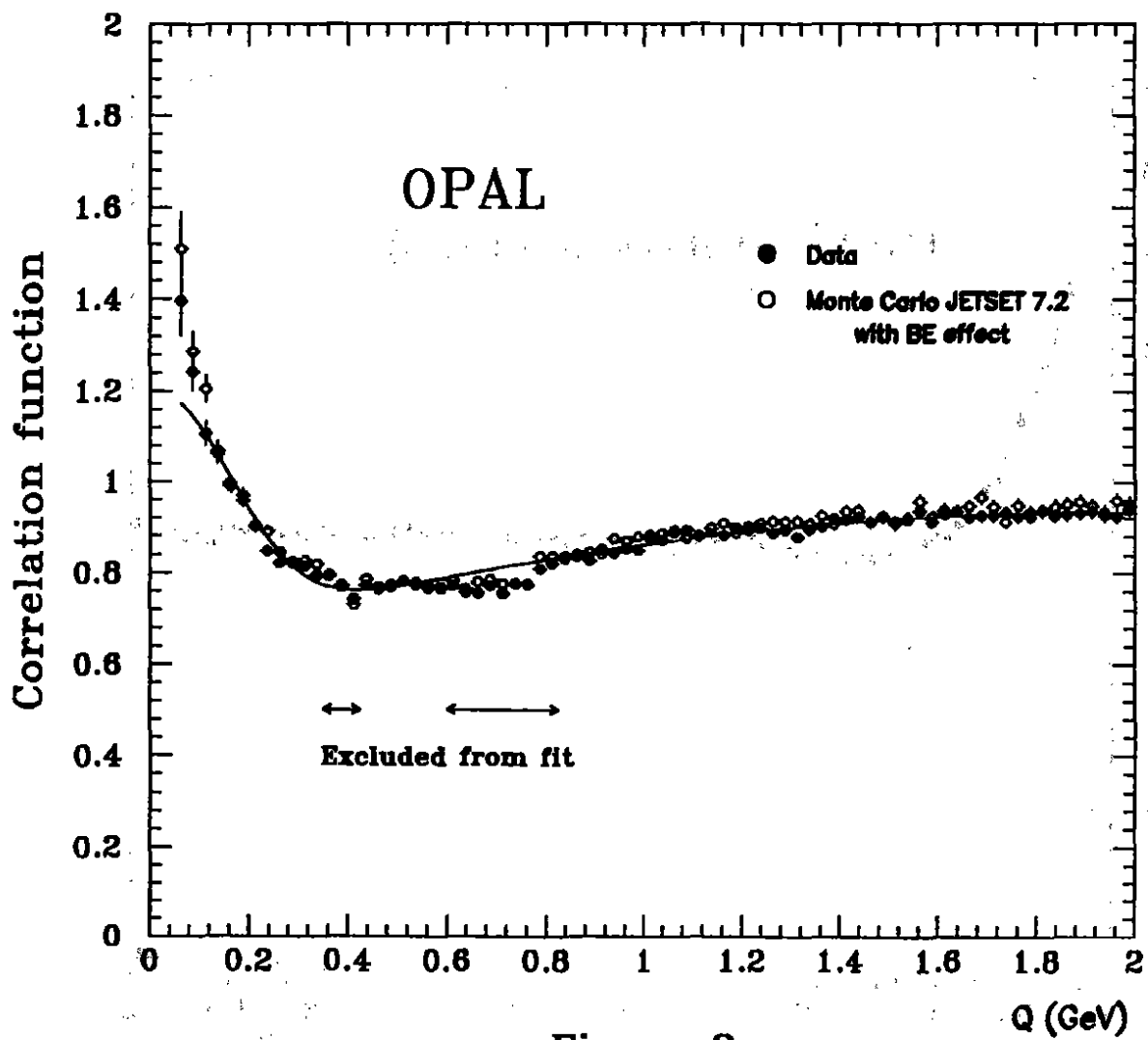


Figure 2

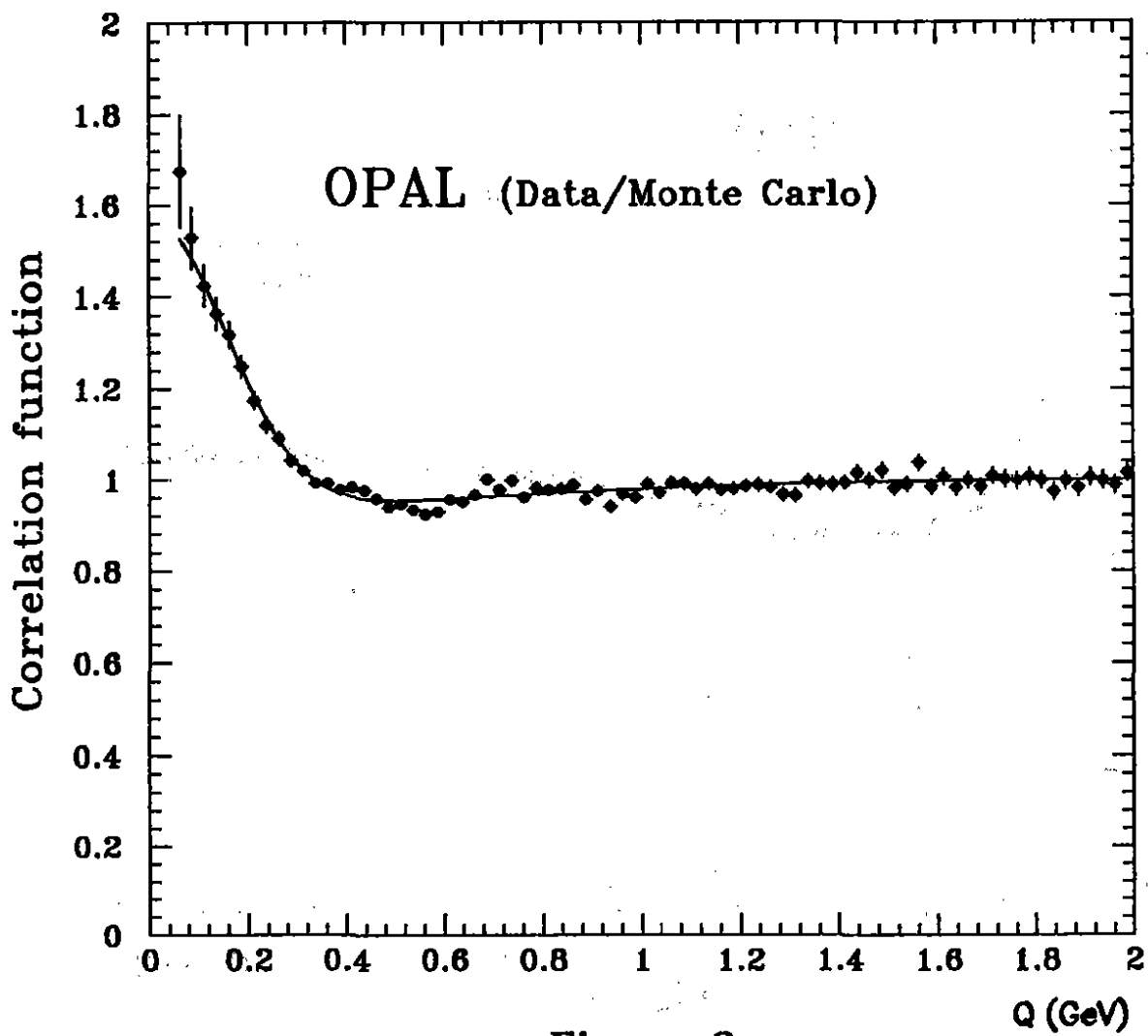


Figure 3

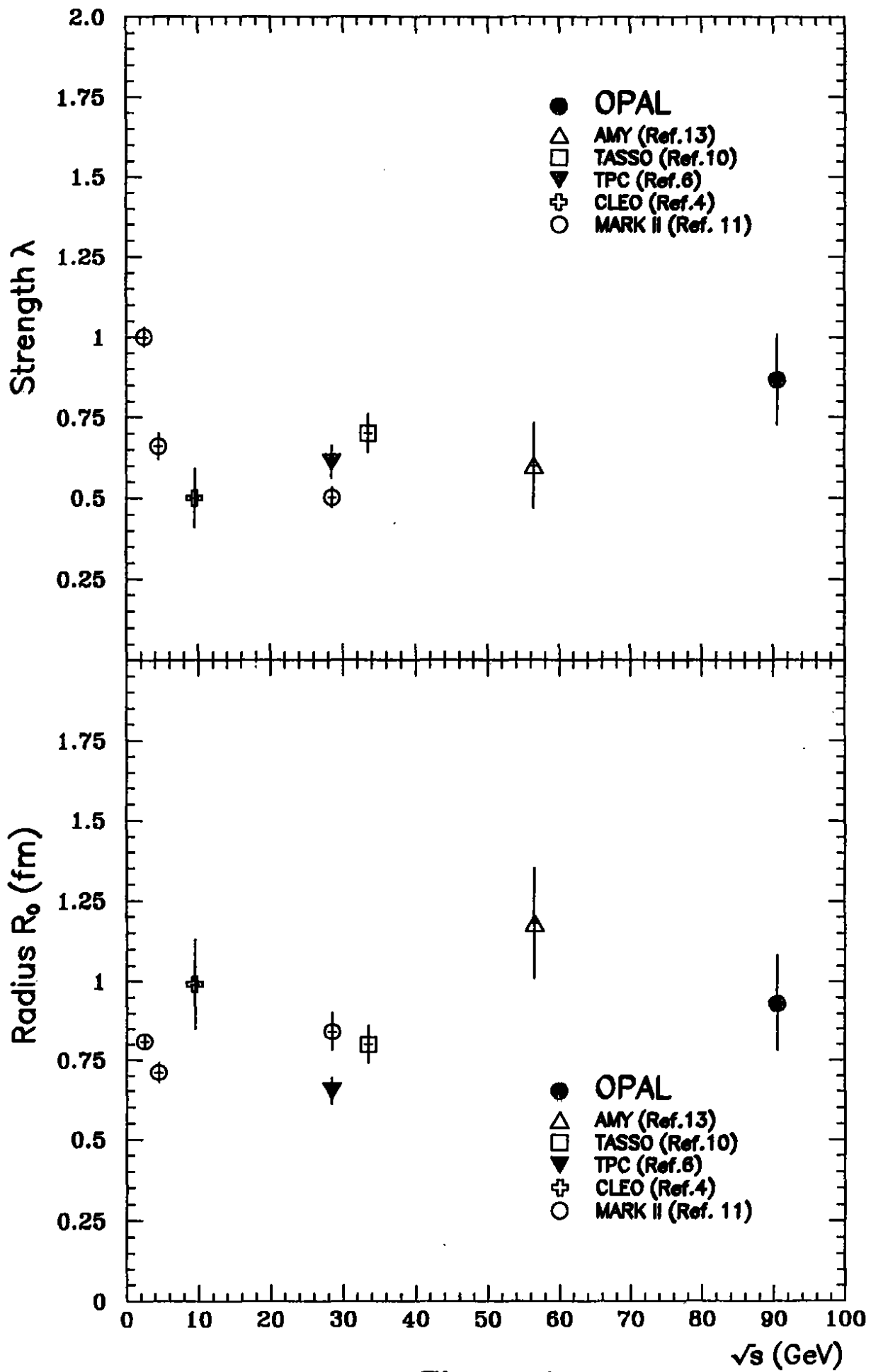


Figure 4